

# Optical length-change measurement based on an incoherent single-bandpass microwave photonic filter with high resolution

Ye Deng, Ming Li,\* Ningbo Huang, Hui Wang, and Ninghua Zhu

State Key Laboratory on Integrated Optoelectronics, Institute of Semiconductors, Chinese Academy of Sciences, Beijing 100083, China

\*Corresponding author: ml@semi.ac.cn

Received April 2, 2014; revised April 29, 2014; accepted May 2, 2014;  
posted June 4, 2014 (Doc. ID 209242); published July 9, 2014

An optical length-change measurement technique is proposed based on an incoherent microwave photonic filter (MPF). The optical length under testing is inserted into an optical link of a single-bandpass MPF based on a polarization-processed incoherent light source. The key feature of the proposed technique is to transfer the length measurement in the optical domain to the electrical domain. In the electrical domain, the measurement resolution is extremely high thanks to the high-resolution measurement of microwave frequency response. In addition, since the MPF is a single-bandpass MPF, the optical length is uniquely determined by the central frequency of the MPF. A detailed investigation of the relation between the center frequency of the MPF and the optical length change is implemented. A measurement experiment is also demonstrated, and the experimental results show that the proposed technique has a measurement sensitivity of 1 GHz/mm with a high length-measurement resolution of 1 pm in theory. The proposed approach has the advantages of high sensitivity, high resolution, and immunity to power variation in electronic and optical links. © 2014 Chinese Laser Press

OCIS codes: (060.5625) Radio frequency photonics; (280.4788) Optical sensing and sensors; (060.2370) Fiber optics sensors; (070.2615) Frequency filtering.  
<http://dx.doi.org/10.1364/PRJ.2.000B35>

## 1. INTRODUCTION

In recent decades, fiber-optic sensing techniques have attracted great interest thanks to the advantages of high sensitivity, fast responsibility, immunity to electromagnetic interference, and intrinsic compatibility with fiber-optic systems [1–3]. Optical length change is one essential measurand that is usually determined by variation in temperature, strain, displacement, distance, or refractive index. Therefore, a great number of approaches have been applied to measure the optical length change, such as fiber gratings, Mach–Zehnder or Sagnac interferometers, optical rings or microrings, and Fabry–Perot cavities [4]. However, the optical length measurement is mainly implemented in the optical domain, which in turn means that the measurement resolution is limited due to the poor interrogation resolution in the optical domain.

Microwave photonic filters (MPFs) have been widely used in the field of optical signal processing, radar, and radio over fiber systems [5–7]. MPFs are photonic subsystems aimed to replace the traditional approach toward radio frequency (RF) signal processing with many advantages, such as large tunability, low loss, electromagnetic immunity, and so on. The key device in an MPF is the optical delay-line module that can be implemented using optical couplers [8,9], fiber Bragg gratings (FBGs) [10–12], Mach–Zehnder lattices [13], arrayed waveguide [14,15], or a length of dispersive fiber [16,17]. Many efforts have been made to achieve tunable MPFs [18–22]. Their applications focus mainly on high-speed signal selecting. However, it is known that MPFs have many other potential applications. Recently, an optical fiber sensor based on RF

Mach–Zehnder interferometers (MZIs) has been experimentally demonstrated [23]. In [23], the proposed sensor has a linear response to an applied temperature change, which can be interrogated using RF instruments. Since the temperature changes are measured in the RF domain, a high resolution measurement is achieved.

In this paper, a single-bandpass MPF-based approach is proposed and experimentally demonstrated to measure optical length change. The key feature of the proposed technique is to transfer the length measurement in the optical domain to the electrical domain. In the electrical domain, the measurement resolution is extremely high thanks to the high resolution measurement of microwave frequency response. In addition, since the MPF is a single-bandpass MPF, the optical length is uniquely determined by the central frequency of the MPF. A detailed investigation of the relation between the center frequency of the MPF and the optical length change is implemented. An experiment is carried out, and the experimental results show that the proposed technique has a measurement sensitivity of 1 GHz/mm with a high length-measurement resolution of 1 pm in theory.

## 2. MEASUREMENT PRINCIPLE

The proposed single-bandpass MPF for the measurement of the optical length change is shown in Fig. 1. The incoherent light emitted from a superluminescent LED (SLED) is reshaped by a tunable optical filter (TOF) with a flat-top filtering window and is polarized by a polarizer (Pol1). The linearly polarized lightwave is sent to a polarization beam splitter

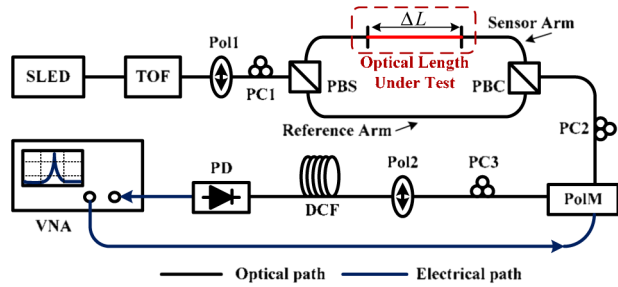


Fig. 1. Schematic showings of the proposed optical length measurement technique based on a single-bandpass MPF. SLED, superluminescent LED; TOF, tunable optical filter; Pol, polarizer; PC, polarization controller; PBS, polarization beam splitter; PBC, polarization beam combiner; PolM, polarization modulator; DCF, dispersion compensation fiber; PD, photodetector; VNA, vector network analyzer.

(PBS) via a polarization controller (PC1) and split into two orthogonally polarized lightwaves. The power of the two orthogonally polarized lightwaves is balanced by adjusting the PC1. One of the two orthogonally polarized lightwaves is directed to the optical length under testing, which is inserted into the sensor arm and then combined with the other one at a polarization beam combiner (PBC). The combined orthogonal lightwaves are sent to a PC2 and aligned at  $\pm 45^\circ$  to one principle axis of a polarization modulator (PolM). Since the PolM is a special phase modulator with opposite modulation indices along two principle axes (x and y axes), the two orthogonal lightwaves (angled at  $\pm 45^\circ$  to the y axis) will be phase modulated inversely by the modulation signal that is generated from a vector network analyzer (VNA).

Mathematically, the output optical field along the x and y principle axes of the PolM can be described as

$$\begin{aligned} \begin{bmatrix} E_x \\ E_y \end{bmatrix} &= \frac{\sqrt{2}}{2} \times \begin{bmatrix} \cos(\pi/4)E_{\text{out1}}(t - \Delta t) \exp[j\beta \cos(\omega_m t)] + \cos(3\pi/4)E_{\text{out1}}(t) \exp[j\beta \cos(\omega_m t)] \\ \sin(\pi/4)E_{\text{out1}}(t - \Delta t) \exp[-j\beta \cos(\omega_m t)] + \sin(\pi/4)E_{\text{out1}}(t) \exp[-j\beta \cos(\omega_m t)] \end{bmatrix} \\ &= \frac{1}{2} \times \begin{bmatrix} E_{\text{out1}}(t - \Delta t) \exp[j\beta \cos(\omega_m t)] & -E_{\text{out1}}(t) \exp[j\beta \cos(\omega_m t)] \\ E_{\text{out1}}(t - \Delta t) \exp[-j\beta \cos(\omega_m t)] & +E_{\text{out1}}(t) \exp[-j\beta \cos(\omega_m t)] \end{bmatrix}, \end{aligned} \quad (1)$$

where  $E_{\text{out1}}(t)$  denotes the output optical field of the Pol1.  $\Delta t = \Delta L/c$  represents the time delay between the sensor arm and the reference arm, and  $\Delta L$  is the optical length difference between the two arms that is defined as the product of its physical length and its refractive index.  $c$  is the light velocity in vacuum.  $\beta$  is the phase modulation index of the PolM, and  $\omega_m$  is the angle frequency of the modulation signal.

The polarization-modulated signal is then sent to a Pol2 that is oriented with the same polarization state of the light in the sensor arm. Therefore, the optical component with a polarization direction parallel with the transmission axis of the Pol2 will pass through, while the other one with a polarization direction vertical to the transmission axis of the Pol2 will be blocked. The output optical field from the Pol2 under a small-signal modulation can be expressed as

$$\begin{aligned} E_{\text{out2}}(t) &= (1/2) \cos(\pi/4) \{ E_{\text{out1}}(t - \Delta t) \exp[j\beta \cos(\omega_m t)] \\ &\quad - E_{\text{out1}}(t) \exp[j\beta \cos(\omega_m t)] \\ &\quad + E_{\text{out1}}(t - \Delta t) \exp[-j\beta \cos(\omega_m t)] \\ &\quad + E_{\text{out1}}(t) \exp[-j\beta \cos(\omega_m t)] \} \\ &\approx (\sqrt{2}/2) J_0(\beta) E_{\text{out1}}(t - \Delta t) \\ &\quad - j\sqrt{2} J_1(\beta) E_{\text{out1}}(t) \cos(\omega_m t), \end{aligned} \quad (2)$$

where  $J_n(\cdot)$  is the  $n$ th-order Bessel function of the first kind ( $n = 0, 1$ ). The Fourier transform of Eq. (2) can be written as

$$\begin{aligned} E_{\text{out2}}(\Omega) &\propto J_0(\beta) E_{\text{out1}}(\Omega) \exp(-j\Omega\Delta t) \\ &\quad - jJ_1(\beta) [E_{\text{out1}}(\Omega - \omega_m) + E_{\text{out1}}(\Omega + \omega_m)]. \end{aligned} \quad (3)$$

From Eq. (3), it can be seen that the phases of the optical carriers  $[E_{\text{out1}}(\Omega)]$  change continuously, which is determined by the time delay of  $\Delta t$ , while the phases of the sidebands  $[E_{\text{out1}}(\Omega \pm \omega_m)]$  stay the same. Thus, a sinusoidal electrical slicing effect will be induced after detection by a photodetector (PD). When the optical length difference  $\Delta L$  is changed, the electrical slicing response will be changed correspondingly.

Afterward, the output optical signal from the Pol2 propagates through a dispersive compensating fiber (DCF) and is detected by a PD. The phase delay  $\Phi(\Omega)$  resulting from the DCF can be approximately written in a Taylor expansion at the center angular frequency ( $\Omega_0$ ) of the filtered incoherent light output from the TOF like [24]

$$\begin{aligned} \Phi(\Omega) &= \Phi(\Omega_0) + \tau(\Omega_0) \cdot (\Omega - \Omega_0) + D \cdot L(\Omega - \Omega_0)^2 / 2 \\ &\quad + \chi \cdot L(\Omega - \Omega_0)^3 / 3, \end{aligned} \quad (4)$$

where  $\tau(\Omega_0)$  is the group delay time,  $D$  is the dispersion, and  $L$  is the length of the DCF. Ignoring the baseband response and the third-order dispersion  $\chi$ , the frequency response of the proposed MPF can be approximately described as [25]

$$\begin{aligned} H(\omega) &\propto H_b(\omega - \Delta t/DL) \exp[j(\Omega_0\Delta t - DL\omega^2/2)] \\ &\quad + H_b(\omega + \Delta t/DL) \exp[j(-\Omega_0\Delta t + DL\omega^2/2)], \end{aligned} \quad (5)$$

where  $H_b(\omega)$  is defined as

$$H_b(\omega) = \frac{1}{2\pi} \int_0^{+\infty} S(\omega) \exp[-j\omega DL(\Omega - \Omega_0)] d\Omega, \quad (6)$$

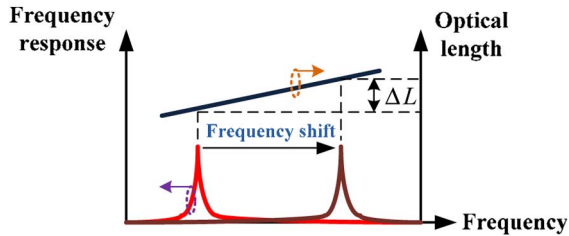


Fig. 2. Basic implementation principle of the proposed MPF-based approach for measuring optical length change.

where  $S(\omega)$  is the optical power spectrum density of the filtered incoherent light source. From Eq. (5), we can see that the  $H(\omega)$  represents a transfer function of a single-bandpass filter and the bandpass center of the proposed MPF can be expressed by

$$f_c = \Delta t / (2\pi DL) = \Delta L / (2\pi c DL). \quad (7)$$

It can be seen from Eq. (7) that a linear relationship is established between the optical length difference and the center frequency of the MPF. The central microwave frequency is uniquely determined by the optical length change, as shown in Fig. 2. Therefore, by interrogating the central microwave frequency, the optical length change could be measured. The measurement resolution of the central microwave frequency determines the measurement resolution of the optical length change.

In addition, the MPF has only one bandpass response, and the measurement range is only limited by the bandwidth of the components in the system, such as the modulator and PD. The change of the optical length difference between the sensor arm and the reference arm reveals the shift of the center frequency of the MPF. Therefore, by tuning the optical length in the reference arm, the measurement range of the optical length in the sensor arm can be extended correspondingly. However, this approach is limited by the tuning precision of the optical length in the reference arm if continual tunability is required. Furthermore, the proposed approach is sensitive to the instability of the reference arm. The environmental fluctuations due to temperature or strain variation in the reference arm may result in unpredictable optical length change. A length-extended reference arm may induce large instability, and thus it may restrict the measurement accuracy.

### 3. EXPERIMENT RESULTS

An experiment based on the single-bandpass MPF is implemented to measure the optical length, as shown in Fig. 1. A SLED (Thorlabs s5fc1005s) cascaded with a TOF (Yenista XTA-50) is employed as the incoherent light source. As shown in Fig. 3, a linearly polarized lightwave with a span of 5 nm that is measured by an optical spectrum analyzer (Advantest Q8384A) is sent to the PBS via the PC1 to split into two orthogonally polarized lightwaves. The power ratio between the two orthogonally polarized lightwaves is set to be 1 by adjusting the PC1. An optical variable delay line (OVDL) is inserted into the sensor arm to emulate the optical length change. The two orthogonally polarized lightwaves are combined at the PBC and then are sent to the PolM with a 3 dB bandwidth of 40 GHz. A sinusoidal microwave signal from the

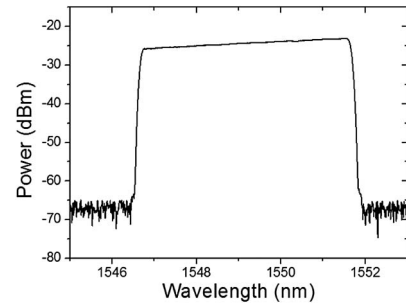


Fig. 3. Measured optical spectrum of the lightwave output from a SLED cascaded with a TOF.

VNA (Agilent 8720D) is applied to the PolM with a frequency sweeping from 50 MHz to 20 GHz. The power of the signal is fixed at 10 dBm. The PC2 and PC3 are used to adjust the angle of the orthogonally polarized optical fields. A DCF with a dispersion value of 425 ps/nm is used to map the modulated optical spectrum into the time domain. Through optical-to-electrical conversion at the PD with a 3 dB bandwidth of 18 GHz, the output RF signal is fed back to the VNA for frequency response measurement.

According to Eq. (7), when the optical length difference  $\Delta L$  is tuned by the OVDL, the center frequency of the MPF will vary linearly with  $\Delta L$ . The experimental results are shown in Fig. 4(a). By tuning the optical length difference from 0 to 12 mm between the two arms, it can be seen that the center frequency of the passband shifts from 2 to 14 GHz. Figure 4(b) shows the frequency responses as the center frequency is tuned around 10 GHz, and its zoom-in view is shown in the inset. It is worth noting that the 3 dB bandwidth of the passband increases as the center frequency becomes higher. This effect results from the third-order dispersion of the DCF. To

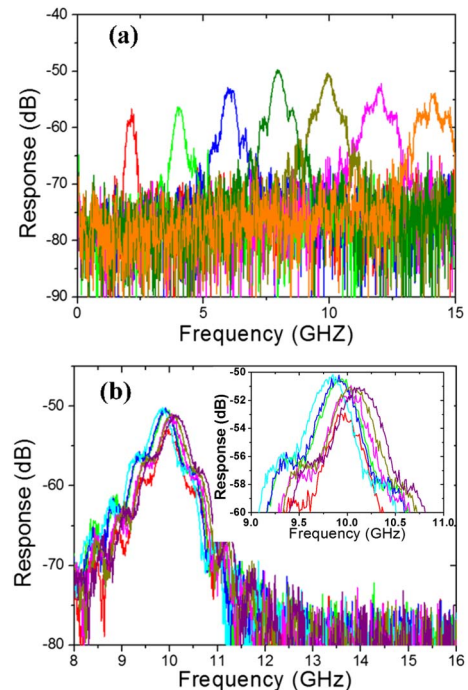


Fig. 4. Measured frequency response of the MPF along with the change of optical length. (a) Center frequency is tuned ranging from 2 to 14 GHz. (b) Center frequency is tuned around 10 GHz.

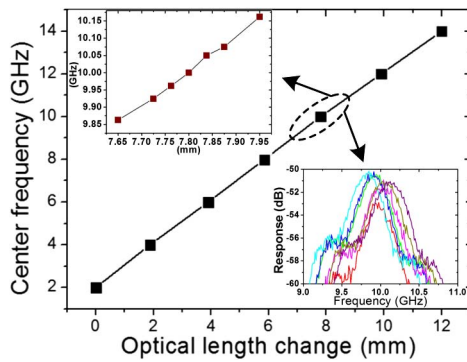


Fig. 5. Relationship between the center frequency of the MPF and the optical length change.

overcome the undesirable effect, a low third-order dispersion medium such as a linear chirped FBG could be used. It also can be observed that the sidelobe suppression ratio is not identical when the passband moves to a higher frequency. This problem could be fixed by adjusting the PC accordingly.

The experimental result shown in Fig. 5 verifies the linear relationship between the center frequency of the MPF and the optical length change. A slope of 1 GHz/mm is obtained, which agrees well with the theoretical results. Here, the sensing sensitivity corresponds to the slope with a value of 1 GHz/mm. More details are shown in the top inset of Fig. 5. A zoom-in view for the range from 7.65 to 7.95 mm is presented, and the local linear relationship agrees well with the total linear relationship. In our experiment, a VNA with a frequency resolution of 1 Hz is used, and thus a resolution to optical length measurement is estimated theoretically to be 1 pm. In an actual measurement, the measurement resolution is largely influenced by the center frequency fluctuation, the noise of the MPF, and the undesired third-order dispersion. For relieving the effect of the center frequency fluctuation, a stable reference arm should be employed. For reducing the influence of the noise in the passband to measure the center frequency accurately, some mathematical calculating methods may be used to smooth the frequency-response curve. The undesired third-order dispersion may broaden the passband as the center frequency became higher, and it also would affect the measurement accuracy of the center frequency. By employing a low third-order dispersion medium such as a linear chirped FBG, this undesirable effect could be suppressed. It should be noted that the OVDL is employed as the emulator for the optical length change by adjusting the physical length, so the measured optical length change above is actually the displacement in air (the refractive index is assumed to be 1). We recall that the optical length change is defined as the product of the physical length change of optical links and the change in refractive index. Therefore, other parameters resulting in optical length change such as temperature, strain, and refractive index can be measured using the proposed MPF. In addition, because the approach extracts the information on optical length change by way of frequency coding and decoding, not intensity information, the measurement result is immune to time-variable or spatial-variable loss of the links.

#### 4. CONCLUSION

An optical length-change measurement technique was proposed based on an incoherent MPF. The optical length under

testing was inserted into an optical link of a single-bandpass MPF based on a polarization-processed incoherent light source. The key feature of the proposed technique is to transfer the length measurement in the optical domain to the electrical domain. In the electrical domain, the measurement resolution is extremely high thanks to the high measurement of the microwave frequency response. In addition, since the MPF is a single-bandpass MPF, the optical length is uniquely determined by the central frequency of the MPF. A detailed investigation of the relation between the center frequency of the MPF and the optical length change was implemented. A measurement experiment was also demonstrated with a measurement sensitivity of 1 GHz/mm and a high length measurement resolution of 1 pm in theory.

#### ACKNOWLEDGMENTS

This work was supported by the National Natural Science Foundation of China under 61377002, 61321063, and 61090391. Ming Li was supported in part by the Thousand Young Talent program.

#### REFERENCES

1. B. Culshaw, "Fiber optics in sensing and measurement," *IEEE J. Sel. Top. Quantum Electron.* **6**, 1014–1021 (2000).
2. B. Lee, "Review of the present status of optical fiber sensors," *Opt. Fiber Technol.* **9**, 57–79 (2003).
3. C. K. Kirkendall and A. Dandridge, "Overview of high performance fibre-optic sensing," *J. Phys. D* **37**, R197 (2004).
4. B. Culshaw and A. Kersey, "Fiber-optic sensing: a historical perspective," *J. Lightwave Technol.* **26**, 1064–1078 (2008).
5. R. A. Minasian, "Photonic signal processing of microwave signals," *IEEE Trans. Microwave Theor. Tech.* **54**, 832–846 (2006).
6. J. Yao, "Microwave photonics," *J. Lightwave Technol.* **27**, 314–335 (2009).
7. J. Capmany, J. Mora, I. Gasulla, J. Sancho, J. Lloret, and S. Sales, "Microwave photonic signal processing," *J. Lightwave Technol.* **31**, 571–586 (2013).
8. E. C. Heyd and R. A. Minasian, "A solution to the synthesis problem of recirculating optical delay line filter," *IEEE Photon. Technol. Lett.* **6**, 833–835 (1994).
9. J. Capmany and J. Martin, "Solutions to the synthesis problem of optical delay line filters," *Opt. Lett.* **20**, 2438–2440 (1995).
10. G. Yu, W. Zhang, and J. A. R. Williams, "High-performance microwave transversal filter using fiber Bragg grating arrays," *IEEE Photon. Technol. Lett.* **12**, 1183–1185 (2000).
11. D. Pastor, J. Capmany, and B. Ortega, "Broad-band tunable microwave transversal notch filter based on tunable uniform fiber Bragg gratings as slicing filters," *IEEE Photon. Technol. Lett.* **13**, 726–728 (2001).
12. W. Zhang, J. A. R. Williams, and I. Bennion, "Polarization synthesized optical transversal filter employing high birefringence fiber gratings," *IEEE Photon. Technol. Lett.* **13**, 523–525 (2001).
13. T. A. Cusick, S. Iezekiel, R. E. Miles, S. Sales, and J. Capmany, "Synthesis of all-optical microwave filters using Mach-Zehnder lattices," *IEEE Trans. Microwave Theor. Tech.* **45**, 1458–1462 (1997).
14. D. Pastor, J. Capmany, and B. Ortega, "Experimental demonstration of parallel fiber-optic-based RF filtering using WDM techniques," *IEEE Photon. Technol. Lett.* **12**, 77–78 (2000).
15. V. Polo, B. Vidal, J. L. Corral, and J. Marti, "Novel tunable photonics microwave filter based on laser arrays and N × N AWG-based delay lines," *IEEE Photon. Technol. Lett.* **15**, 584–586 (2003).
16. D. Norton, S. Johns, C. Keefer, and R. Soref, "Tunable microwave filtering using high dispersion fiber time delays," *IEEE Photon. Technol. Lett.* **6**, 831–832 (1994).
17. K. H. Lee, W. Y. Choi, S. Choi, and K. Oh, "A novel tunable fiber-optic microwave filter using multimode DCF," *IEEE Photon. Technol. Lett.* **15**, 969–971 (2003).
18. H. Fu, D. Chen, H. Ou, and S. He, "Continuously tunable incoherent microwave photonic filter using a tunable Mach-Zehnder



- interferometer as the slicing filter,” *Microwave Opt. Technol. Lett.* **49**, 2382–2386 (2007).
19. W. Li, M. Li, and J. Yao, “A narrow-passband and frequency-tunable microwave photonic filter based on phase-modulation to intensity-modulation conversion using a phase-shifted fiber Bragg grating,” *IEEE Trans. Microwave Theor. Tech.* **60**, 1287–1296 (2012).
  20. X. Xue, X. Zheng, H. Zhang, and B. Zhou, “Widely tunable single-bandpass microwave photonic filter employing a non-sliced broadband optical source,” *Opt. Express* **19**, 18423–18429 (2011).
  21. W. Li, L. X. Wang, and N. H. Zhu, “All-optical microwave photonic single-passband filter based on polarization control through stimulated Brillouin scattering,” *IEEE Photon. J.* **5**, 5501411 (2013).
  22. H. Wang, J. Y. Zheng, W. Li, L. X. Wang, M. Li, L. Xie, and N. H. Zhu, “Widely tunable single-bandpass microwave photonic filter based on polarization processing of a nonsliced broadband optical source,” *Opt. Lett.* **38**, 4857–4860 (2013).
  23. T. Wei, J. Huang, X. Lan, Q. Han, and H. Xiao, “Optical fiber sensor based on a radio-frequency Mach-Zehnder interferometer,” *Opt. Lett.* **37**, 647–649 (2012).
  24. J. Mora, B. Ortega, A. Díez, J. L. Cruz, M. V. Andrés, J. Capmany, and D. Pastor, “Photonic microwave tunable single-bandpass filter based on a Mach-Zehnder interferometer,” *J. Lightwave Technol.* **24**, 2500 (2006).
  25. X. Yi and R. A. Minasian, “Dispersion induced RF distortion of spectrum-sliced microwave-photonic filters,” *IEEE Trans. Microwave Theor. Tech.* **54**, 880–886 (2006).